RSC Advances

ROYAL SOCIETY OF CHEMISTRY

www.rsc.org/advances

Preparation and absorption behavior to organic pollutants of macroporous hydrophobic polyvinyl alcohol-formaldehyde sponges

Yanxiong Pan,[ab] Chao Peng,[a] Weicai Wang,[ab] Kai Shi,[a] Zhi Liu[a] and Xiangling Ji[*a]

Received (in XXX, XXX) Xth XXXXXXXXX 20XX, Accepted Xth XXXXXXXXX 20XX
DOI: 10.1039/b000000x

[a] *State Key Laboratory of Polymer Physics and Chemistry, Changchun Institute of Applied Chemistry, Chinese Academy of Sciences, Changchun 130022, P.R. of China. E-mail: xlji@ciac.ac.cn*

[b] *University of Chinese Academy of Sciences, Beijing 100039, PR China*.

† Electronic Supplementary Information (ESI) available: Movie of toluene absorption experiments, FTIR and Solid-state CP/MAS ^{13}C-NMR spectra of PVF–G_n-H_ms sponges, Pore size distributions of PVF–G_n-H_ms sponges, The effect of GA feed ratio, alkyl chain length and reaction temperature on the absorption capacity of PVF–G_n-H_ms sponges for various organic solvents. See DOI: 10.1039/b000000x/

Abstract: A series of macroporous hydrophobic polyvinyl alcohol–formaldehyde sponges (PVF–G_n-H_ms) are prepared via the reactions of hydrophilic polyvinyl alcohol–formaldehyde (PVF) sponges with glutaraldehyde (GA) and fatty acyl chloride. Both ATR-IR and solid-state CP/MAS ^{13}C-NMR spectra confirm a successful substitution of alkyl chain on PVF sponges and calculated degree of substitution (DS) is in the range of 32.3-62.3%. PVF-G_n-H_ms sponges have similar apparent densities as the pristine PVF sponges and exhibit a unimodal macropore size distribution with a peak centered at about 60 μm and high porosity of 90%. PVF-G_n-H_ms maintain the original open-cell structure well and their surface hydrophobicity effectively increases with the n-alkyl chain length and reaction temperature. The effect of preparation conditions, including the feed ratio of crosslinker glutaraldehyde to OH groups ([GA]/[OH] = 0-4), alkyl chain length of fatty acyl chloride, reaction temperature and apparent density of pristine PVFs, on absorption behavior to organic pollutants is investigated extensively. Fourteen common solvents with solubility parameters from 7.24 to 13.40 $cal^{1/2}\cdot cm^{-3/2}$ are selected as organic pollutants. Results demonstrate that the resultant PVF-G_n-H_ms with higher feed ratio of [GA]/[OH] (from 0 to 4) possess lower absorption capacities in most organic solvents because of relatively higher crosslinking degree. The sponges prepared at higher reaction temperature only exhibits slightly increased absorption capacities; and relatively lower apparent density of pristine hydrophilic PVF facilitates higher absorption capacities. Definitely, the hydrophobic sponges with different apparent densities exhibit excellent reusability and recovery (up to 93.0%) during 35 successive absorption–squeezing cycles, and excellent absorption selectivity in water-organic solvent mixture experiment. More importantly, as-prepared sponges possess hydrophobic surfaces, open-cell structures, high

porosity, as well as excellent reusability and selectivity, which make them ideal candidates as absorbents for organic pollutants.

Introduction

Intentional and accidental leakage of hydrocarbon products, including oils and organic solvents, in the water medium have led to a catastrophic influence on the living environment of water species and human being.[1-3] Thus, an effective strategy to deal with these pollutants in a timely manner is urgent.

Absorbents with hydrophobic and superhydrophobic surfaces are applied to remove organic pollutants from the water medium.[4-6] Compared with other absorbents, macroporous absorbents possess obvious advantages, such as large pore volume, rapid absorption kinetics, excellent absorption capacity, selectivity and easy reuse. These features have motivated the researchers to study novel macroporous materials with special surface hydrophobicity as effective absorbents for practical application. Although new types of organic absorbents, such as carbon nanotube sponge,[7,8] aerogel,[9-11] butyl rubber,[6, 12-14] magnetic foam,[15] hydrophobic PU foam[5, 16,17] and electrospun fiber,[18-22] have been reported, high cost, strict reaction conditions, and poor reusability limit their large-scale production and practical applications.

Polyvinyl alcohol–formaldehyde (PVF) sponge is a kind of hydrophilic material with open-cell structure, good mechanical properties at low apparent density, as well as outstanding water absorption capacity and excellent biocompatibility.[23] They have been widely used as mops, pads [24,25] and operative implants.[26] The proportion of vinyl alcohol unit in any poly(vinyl acetal) is more than 13.5%,[27,28] which provides possibility to functionalize PVF readily due to rich hydroxyl groups in its network.[29] In our previous work,[29] the macroporous and hydrophobic polyvinyl alcohol-formaldehyde sponges (PVF-GA-Hs) were prepared through PVF (polyvinyl alcohol-formaldehyde) with glutaraldehyde and stearoyl chloride at the ambient temperature. Definitely, as-prepared PVF-Hs possess fast absorption kinetics to organic solvents and can absorb organic solvents up to 94.3 $g.g^{-1}$, excellent reusability, and selectivity. Here, as an extended work we prepared a series hydrophobic PVF sponges through two-step reactions of the hydroxyl groups in PVF with GA and fatty acyl chloride at different temperatures. Preparative conditions, such as feed ratio of [GA]/[OH], alkyl chain length, reaction temperature and pristine PVF apparent density, were investigated extensively, including their influence on the absorption capacities.

Experimental sections

Materials and Regents

Poly (vinyl alcohol) (PVA) powder with degree of polymerization of 2000 and saponification degree of 99% was obtained from Shanxi Sanwei Group Co., Ltd, China. Triton X-100, GA (50% aqueous solution), and fatty acids, including n-butyric acid, n-octanoic acid, lauric acid, palmitic acid and stearic acid, were purchased from Aladdin. Formaldehyde and other reagents were purchased from Beijing Chemical Works and used as received. Fatty acyl chlorides, such as n-butyryl chloride, n-octanoyl chloride, lauroyl chloride, palmitoyl chloride and stearoyl chloride, were prepared using conventional literature methods.[30,31] All other reagents used in this study were of analytical reagent grade and used as received.

Preparation of pristine PVF sponges

Typical preparation of PVF sponge has been reported in the literature[32]. In detail, a certain amount of PVA was dissolved in 450 g deionized water by vigorous stirring with a magnetic stir bar at 95 ºC until complete dissolution. Then, formaldehyde and Triton X-100 were poured into 60 g of hot PVA solution under vigorous stirring. Liquid froths were obtained after 5 min. Then 30 mL of 50 wt% H_2SO_4 was poured into the above froth at room temperature. After reaching maximum volume, the froths were poured into a mold and cured in an oven at 60 ºC for 5 h. The raw samples were washed with water at least five times to remove unreacted reactants. Finally, the sponges were available after drying at 60 ºC to a constant weight. PVF sponges with apparent densities of about 0.059, 0.073, 0.095, and 0.110 $g\cdot cm^{-3}$ were prepared.

Preparation of PVF-G_n sponges

Crosslinking reaction between PVF sponges and GA was carried out in the presence of sulfuric acid as catalyst. Typically, 10 g as-prepared PVF sponges and a certain amount of GA were added into 400 mL sulfuric acid 20 wt% aqueous solution. The mixture was kept at 25 ºC for 24 h. Then, the sample was washed with water to remove sulfuric acid and unreacted GA, and then dried at 60 ºC to a constant weight. PVF-GA was obtained. To investigate the influence of GA amount on the absorption capacity of hydrophobic PVFs in organic solvents, the feed ratio of [GA]/[OH] was varied in the range of 0/1 to 4/1 in molar ratio (as determined by ^{1}H-NMR). The resulting samples were denoted as PVF-G_n (where *n* is the feed ratio of [GA]/[OH]).

Preparation of hydrophobic PVF-G_n-H_m sponges

A series of hydrophobic PVF sponges were prepared under different conditions, such as fatty acyl chloride with different alkyl chain lengths, reaction temperatures, feed ratios of [GA]/[OH] and pristine apparent densities of PVF. Typically, 5 g PVF-G_n was cut into small pieces (10 × 10 × 50 mm^3) and immersed into a mixed solution of 100 mL acetonitrile and a stoichiometric amount (relative to hydroxyl group in PVF sponges) of stearoyl chloride (C_{18}) at 25, 50, and 75 ºC for 24 h. The resulting samples were denoted as PVF-G_n-H_{18}, PVF-G_n-H_{18} (50), and PVF-G_n-H_{18} (75). The samples were washed thoroughly with toluene and dried in a vacuum oven at 50 ºC. The PVF modified with other fatty acyl chlorides underwent the same procedure (for n-butyryl chloride (C_4), n-octanoyl chloride (C_8), n-dodecanoyl chloride (C_{12}), and n-palmitoyl chloride (C_{16})), and denoted as PVF-G_n-H_m (where m is carbon number of fatty acyl chloride). The PVF sponges with different pristine apparent densities were denoted as PVF-G_n-H_m-ρ (where ρ is the value of apparent density of pristine PVF sponges).

Characterization of the PVF sponges

Fourier transform infrared spectrum was performed on a Bruker Vertex 70 spectrometer with attenuated total reflection (ATR) attachment. Solid-state CP/MAS ^{13}C-NMR spectra were recorded on Bruker AV-400-WB spectrometer. Surface morphology was observed using field emission environmental scanning electron microscopy (FE-SEM) (Micro FEI Philips XL-30-ESEM-FEG) operating at 15 kV. Water contact angle was measured using Krüss DSA10-MK2 drop shape analyzer at ambient temperature using water as probe liquid (3 μL). Pore size and porosity were obtained by automatic intrusion porosimeter (Autopore IV 9500, Micromeritics, USA).

The apparent density of the as-prepared PVFs was measured as follows. The PVF monoliths were cut into small pieces (about 40 × 40 × 15 mm^3). The weights of PVF specimens were obtained using an analytical balance, and the volumes of specimens were measured directly. The apparent density of PVF was calculated as follows.

$$\rho = W_0 / V_0$$

where W_0 is the weight of dried PVF and V_0 is the volume of dried PVF. The final result was the average of three individual specimens.

Absorption performance of sponges

Different organic solvents with various polarities and densities were used for the absorption tests at room temperature, including n-hexane, 1,4-dioxane, carbon tetrachloride, benzene, dimethyl benzene, toluene, anisole, chloroform, chlorobenzene, THF, dichloromethane, nitrobenzene, DMF and DMSO (see SI Table S1). Typically, the dry sponges were cut into dimensions of 10 × 10 × 5 mm^3 and immersed into 200 mL solvents for 30 seconds in order to facilitate the testing even the absorption equilibrium could be reach within 5 seconds. Then, they were taken from the solvents. The weights of the wet sponges were determined after being drained for 0.5 min in stainless mesh. The saturated absorption capacity was defined as

$$Q_s = (W_s - W_0)/W_0 \qquad (1)$$

where W_0 is the dry sponge mass (g) and W_s is the wet sponge mass (g) after solvent absorption.

The volume swelling ratio (Q_v) of as-prepared samples in various organic solvents with various solubility parameters was also calculated from the saturated absorption capacity and defined as follows.

$$Q_v = (W_s/\rho_s + W_0/\rho_0)/W_0/\rho_0 \qquad (2)$$

where W_s is the weight of absorbed organic solvents at saturated state of samples in various organic solvents and ρ_s and ρ_0 are the apparent densities of the organic solvent and the dried sample, respectively.

Reusability of sponges and recovery of organic solvents

The reusability of sponges was achieved by simple mechanical squeezing, and the absorbed organic solvents were recovered from the samples. The recovery (R_e) of various organic solvents were calculated as

$$R_e = W_{re}/(W_e - W_0) \qquad (3)$$

where W_{re} is the mass of recovered organic solvents, W_0 is the dry sponge mass (g), and W_e is the wet sponge mass (g) at absorption equilibrium state. The squeezed sponge was reused for successive absorption–desorption experiment (35 cycles for each sample).

Removal of organic solvents from the mixture

The PVF-H sponges serve as effective absorbents in the direct removal of organic solvents from water-organic solvent mixtures. Typically, 10 mL organic solvents were poured into 300 mL tap water in a 200 mL glass beaker. Then, the PVF-H sponge (about 10 × 10 × 20 cm^3) was placed on top of the mixture.

Results and discussion

Characterization of chemical structure, degree of substitution and pore structures

The synthetic route of a series of macroporous hydrophobic PVF–G_n-H_m sponges is illustrated in Scheme 1. Generally, it includes two steps, the first is the preparation of PVF-G_n via acetalization reaction of GA with hydroxyl groups of PVF, the second is reaction of the residue hydroxyl groups in PVF network with fatty acyl chloride. Here, n = 0 imply the hydroxyl group of PVF reacted with fatty acyl chloride directly without further acetalization with GA. The characterization of chemical structure, apparent density, porosity, pore size and distribution of sponges before and after modification are described extensively in the supporting information (SI) and shown in Table 1. Briefly, both ATR-IR and CP/MAS ^{13}C NMR spectra confirm a successful substitution of alkyl chain (C_4-C_{18}) on PVF sponges and calculated degree of substitution (DS) is in the range of 32.3-62.3%. The apparent density of hydrophobic PVF-G_n-H_m sponge is similar to the initial hydrophilic PVF sample. Most samples exhibit a unimodal macropore size distribution with a peak centered at about 60 μm and high porosity of 90%.

The open-cell structures and macroscopically rough surface are also confirmed using SEM images as shown in Fig. 1. PVF-G_1-H_4, PVF-G_1-H_{18}, and PVF-G_1-H_{18}-0.110 possess open cells with hierarchical pore structures. The two-step substitution of the hydroxyl groups in PVF sponges with GA and fatty acyl chloride still retains the original pore size distribution and the high porosity of pristine PVF, which will finally contribute to high absorption performance for organic solvents.

Change of surface property

As shown in Table 1 and in the inset of Fig. 1, the surface wettabilities of PVF sponges before and after modification were determined by the drop shape analyzer using water as probe liquid (3 μL). The effect of alkyl chain length on surface hydrophobicity of PVF-G_1-H_ms was also investigated. The water contact angles of PVF-G_1-$H_{4\sim18}$ modified with butyryl chloride, octanoyl chloride, dodecanoyl chloride, and stearoyl chloride at 25 ºC are 123.6 ± 0.9°, 124.7 ± 0.8°, 130.5 ± 0.5°, 131.8 ± 1.3°, and 133.5 ± 0.5°, respectively, indicating that the surface hydrophobicity effectively increases with the n-alkyl chain length. The water contact angles of PVF-G_1-H_{18} prepared at 25, 50, and 75 ºC are 133.5 ± 0.5°, 136.4 ± 0.6°, and 138.3 ± 0.7°, respectively, suggesting the higher hydrophobicity available at higher reaction temperature. The introduction of GA at the first step has almost no influence on the contact angle of as-prepared PVF-G_0-H_{18}, PVF-G_1-H_{18}, PVF-G_2-H_{18}, and PVF-G_4-H_{18} (132°–133°). By contrast, the water contact angles of PVF-G_1-H_{18}-0.059, PVF-G_1-H_{18}-0.073, PVF-G_1-H_{18}-0.095, and PVF-G_1-H_{18}-0.110 are 133.1 ± 1.5°, 133.5 ± 0.5°, 135.3 ± 1.3°, and 136.2 ± 0.8°, respectively, indicating that the preparation of hydrophobic PVFs can be realized even for those with high apparent densities due to their high porosity.

Absorption performance of PVF sponges in various organic solvents

The swelling process of crosslinked macroporous polymer involves the rapid diffusion of the solvents into the pores; the polymer chains take up solvents from the environment,[33,34] which is determined by the porosity and the nature of the polymer chains. The structural characteristics of the hydrophobic samples, including hydrophobicity, interconnected pore structures, high porosity and good mechanical properties at low-density, are all beneficial to the swelling of samples in weak polar organic solvents, which could rapidly fill in macroporous PVFs via a capillary effect. Then, the absorbents could reach absorption equilibrium within 5 seconds (See SI, Movie 1). Fourteen organic solvents with different solubility parameters were employed to investigate the influence of the crosslinking degree of PVFs, alkyl chain length, acylation reaction temperature, and apparent density of pristine sponges on absorption performance of as-prepared samples, as described in the following four parts. The reasons induced the change of absorption performance are also discussed.

Absorption capacity with feed ratio of [GA]/[OH]

As mentioned in the experimental section, the feed ratio of [GA]/[OH] was fixed at 0/1, 1/1, 2/1, and 4/1, respectively. The samples were designated as PVF-$G_{0\text{-}4}$-H_{18}s. The saturated absorption capacity of resultant sponges in various organic solvents is shown in Fig. 2a. For example, the absorption capacities of PVF-$G_{0\text{-}4}$-H_{18}s in THF are 62.7, 51.9, 37.0, and 28.0 $g \cdot g^{-1}$， respectively. In nitrobenzene, the values are 101.5, 51.9, 41.1, and 37.0 $g \cdot g^{-1}$, respectively. The absorption capacities in both THF and nitrobenzene decrease with the feed ratio of [GA]/[OH], as shown in Fig. 2b. The same trend can be found in the following solvents, CCl_4, dimethyl benzene, toluene, anisole, benzene, chloroform, chlorobenzene, dichlorobenzene, and 1,4-dioxane. PVF-$G_{0\text{-}4}$-H_{18}s show very low Qs of 6.9-16.0 g·g^{-1} in n-hexane, DMSO and DMF (Figs. 2a and see SI Fig S4). And there is no evident trend with the feed ratio.

Generally, the swelling kinetics is mainly controlled by the skeleton composition and pore channels of porous materials,[14, 33] and the swelling degree is related to the difference of solubility parameters between polymer and solvents.[35,36] To clarify the mechanism of high Q_s of samples, we measured the volume swelling ratio in various organic solvents with different solubility parameters. As shown in Fig. 2c, the maximum volume swelling ratio of PVF-$G_{0\text{-}4}$-H_{18}s was observed in THF, which has a solubility parameter of 9.52 (cal·cm^{-3})$^{1/2}$. This value (9.52 (cal·cm^{-3})$^{1/2}$) can be considered as the solubility parameter of PVF-$G_{0\text{-}4}$-H_{18}s. In Fig. 2c, we can also find that the swelling ratio decreases substantially with the feed ratio of [GA]/[OH]. The presence of more GA in the reaction system leads to higher crosslinking degree, which gives rise to low pore volume expansion during swelling. Thus, the decrease in absorption capacities with feed ratio of [GA]/[OH] comes from higher crosslinking degree of sponges.

Absorption capacity with alkyl chain length

The effect of hydrophobic n-alkyl chain length on absorption capacity of samples in various organic solvents was investigated. PVF-G_1 substituted with variable fatty acyl chloride at 25 ºC includes butyryl chloride (PVF-G_1-H_4), octanoyl chloride (PVF-G_1-H_8), dodecanoyl chloride (PVF-G_1-H_{12}), palmitoyl chloride (PVF-G_1-H_{16}) and stearoyl chloride (PVF-G_1-H_{18}),. Their absorption performances are illustrated in Fig. 3a and S5.

PVF-G_1-H_4, PVF-G_1-H_8, PVF-G_1-H_{12}, PVF-G_1-H_{16}, and PVF-G_1-H_{18} exhibit different absorption properties in various solvents, as shown in Fig. 3b. In nonpolar solvents, such as n-hexane, their absorption capacities Q_s are 8.7, 8.8, 12.3, 13.6, and 14.2 $g\cdot g^{-1}$; In less polar solvents, such as chloroform, Q_s are 41.2, 74.4, 83.0, 83.6, and 89.3 $g\cdot g^{-1}$. PVF-G_1-H_{18} exhibits relatively higher absorption capacities in less polar solvents than in nonpolar solvents. Whether in less polar solvents or in nonpolar solvents, the absorption capacities increase with alkyl chain length. Thus, the absorption capacities of samples in nonpolar solvents and less polar solvents are summarized in the following order: PVF-G_1-H_4 < PVF-G_1-H_8 < PVF-G_1-H_{12} < PVF-G_1-H_{16} < PVF-G_1-H_{18}.

In strong polar solvents, such as DMF and DMSO (see SI Fig S5), the absorption capacities of PVF-G_1-$H_{4\text{-}18}$ are in the range of 8.0 $g\cdot g^{-1}$ to 38.1 $g\cdot g^{-1}$. These values are relatively lower than those in other solvents. No a gradual increase can be observed with increasing chain length.

The above results can be explained using the solubility parameters of samples obtained from the swelling experiment, as shown in Fig. 3c. The maximum volume swellings of PVF-G_1-H_4, PVF-G_1-H_8, PVF-G_1-H_{12}, PVF-G_1-H_{16}, and PVF-G_1-H_{18} are obtained in dichloromethane (9.73 $(cal\cdot cm^{-3})^{1/2}$), dichloromethane (9.73 $(cal\cdot cm^{-3})^{1/2}$), chlorobenzene (9.57 $(cal\cdot cm^{-3})^{1/2}$), chlorobenzene (9.57 $(cal\cdot cm^{-3})^{1/2}$), and THF (9.52 $(cal.\ cm^{-3})^{1/2}$), respectively, corresponding to maximum volume swelling ratios of 2.65, 4.28, 5.13, 4.88, and 5.33, respectively, indicating that the PVF-G_1-H_m with longer alkyl chain has relatively lower solubility parameter but higher swelling ratio. The water contact angles changing from 123.6° to 133.5°confirm that the hydrophobicity of samples increases slightly with alkyl chain length. Thus, the above results indicate that the alkyl chain length has positive effect on improving the Qs of samples, which is mainly attributed to the long alkyl chain increasing hydrophobicity of specimens and solvation degree in these solvents.

Absorption capacity with reaction temperature

The substitution of hydroxyl groups in PVF sponge with stearoyl chloride was carried out at 25 ºC (PVF-G_1-H_{18}), 50 ºC (PVF-G_1-H_{18}-(50)), and 75 ºC (PVF-G_1-H_{18}-(75)). The corresponding absorption performance is presented in Fig. 4a-b and (see SI Fig S6). In Fig. 4b, the absorption capacities of PVF-G_1-H_{18}, PVF-G_1-H_{18}-(50), and PVF-G_1-H_{18}-(75) in nitrobenzene are 51.9, 45.5, and 47.0 $g \cdot g^{-1}$, whereas their Q_s in dimethyl benzene are 41.6, 43.6, and 46.5 $g \cdot g^{-1}$, respectively. Increasing reaction temperature only leads to a very slight increase of absorption capacities in n-hexane, dimethyl benzene, toluene, anisole, benzene, and dichloromethane. In the polar solvents, their absorption capacities in DMSO are 8.3, 8.6, and 9.2 $g \cdot g^{-1}$, whereas their Q_s in DMF are 11.2, 11.8, and 10.9 $g \cdot g^{-1}$, respectively. However, in CCl_4, chloroform, THF, chlorobenzene, dioxane, nitrobenzene, DMF, and DMSO, no obvious change was observed in the absorption capacities with reaction temperature.

As shown in Fig. 4c, the three PVF-G_1-H_{18} sponges prepared at 25, 50, and 75 ºC almost have the same solubility parameter of 9.52 $(cal.\ cm^{-3})^{1/2}$. Thus, the higher Qs of the sample prepared at 75 ºC arises from the high degree of substitution of 62.3%, which contributes to the high solvation degree of PVF-Hs in less-polar and nonpolar solvents.

Absorption capacity with pristine apparent density

Generally, absorbents with lower apparent density exhibit relatively higher absorption performance under the same testing condition. As-prepared hydrophobic PVF-G_1-H_{18} sponges with different pristine apparent densities of 0.059, 0.073, 0.095, and 0.110 $g \cdot cm^{-3}$ were immersed in toluene for a few seconds, and then the mass of wet sponges was measured. As shown in Fig. 5, the absorption capacities in toluene are 48.7, 43.1, 32.4, and 31.0 $g \cdot g^{-1}$, respectively, indicating that the sponge with lower apparent density has higher *Q*s in solvents. Similar result has been reported in the literature.[4,5] The saturated absorption capacities for pollutants decrease with the increasing apparent density of absorbents. The above four samples have DS of 55.3%, 54.1%, 57.8%, and 60.8%. DS only increases slightly with pristine apparent density. Generally, high DS facilitates high *Q*s, but the sponge with apparent density of 0.110 $g\cdot cm^{-3}$ has the lowest absorption capacities. These four samples have the similar porosity of 90% and solubility parameter of 9.52 $(cal.\ cm^{-3})^{1/2}$. Thus, we considered that the higher Q_s of sponges with lower apparent density is related to higher pore volume during the swelling experiment, i.e., the solvent will occupy the bigger pore volume for the sponge with lower apparent density.

Reusability, recovery and selectivity

Adebajo and colleagues extensively reviewed the characteristic of ideal absorbents for oil spills, including oleophilicity and hydrophobicity, high rate and capacity of uptake, absorption selectivity, and absorbed oil could be recovered from absorbents. In fact, the reusability of absorbents and the recovery of pollutant are also key criteria for practical applications.[4]

In our previous study, the PVF-GA-H samples exhibit excellent reusability and separation of organic solvent from water body.[29] As mentioned above, PVF-G_n-H_m sponges exhibit excellent absorption performance in various organic solvents, such as controllable hydrophobicity and high absorption capacities. To demonstrate its reusability, PVF-G_1-H_{18}s with different apparent densities were selected as testing samples, immersed into toluene, and then underwent 35 successive absorption–squeezing cycles. The repeat Q_s and recovery of PVF-G_1-H_{18}s for toluene are shown in Fig. 6.

Interestingly, all PVF-G_1-H_{18}s during repeated absorption cycles possess slightly higher absorption capacities than static absorption, as shown in Fig. 6. For example, the absorption capacities of PVF-G_1-H_{18}-0.059, PVF-G_1-H_{18}-0.073, PVF-G_1-H_{18}-0.095, and PVF-G_1-H_{18}-0.110 during repeated cycles are 48.7, 43.5, 32.4, and 31.0 $g.g^{-1}$, respectively, whereas the absorption capacities at static process are 48.5, 43.1, 30.6, and 29.5 $g.g^{-1}$, respectively. These results may be attributed to more toluene filling into the pore channels during the squeezing process, which pushes residue-entrapped air out of the PVF-G_1-H_{18}s network. Compared with dried PVF-G_n-H_m that requires a few seconds to reach absorption equilibrium, the wet PVF-H could reach absorption equilibrium instantly once the sponges go in contact with toluene. This advantage benefits the practical application of these sponges at emergency situations, such as chemical leakages and oil spills.

As shown in Fig. 6b, the recoveries of PVF-G_1-H_{18}-0.059, PVF-G_1-H_{18}-0.073, PVF-G_1-H_{18}-0.095, and PVF-G_1-H_{18}-0.110 in toluene are 93.0%, 92.0%, 92.0%, and 89.3%, respectively. The absorbed toluene can be collected easily by simple squeezing, which is attributed to the connected pore structure and high porosity of this kind of sponges.

In Fig. 7, the selected absorption experiment in toluene-water mixture is shown. The floating toluene is easily collected by as-prepared sponges and then recovered by simple squeezing. Once the samples go in contact with the organic solvents, they would swell rapidly and reach equilibrium state within a few seconds. Owing to the hydrophobic surface and low apparent density of the sample, the tested samples before and after absorption float on the water surface, easily removing pollutants by taking out the swollen sample. Visual observation demonstrates that there was almost no water in the recovered toluene, indicating the good absorption selectivity of sample in the toluene-water mixture. The above recycling experiment proves that PVF-G-H sponges exhibit excellent reusability due to good mechanical properties at dry and wet states, which can undergo large compressive deformation without any damage.

Conclusions

A series of macroporous hydrophobic PVF-G_n-H_m sponges is prepared successfully via the reactions of hydrophilic PVFs with glutaraldehyde and fatty acyl chloride. The absorption performance of sponges in fourteen common solvents is determined to a large extent by the preparation conditions, including feed ratio of [GA]/[OH], alkyl chain length, reaction temperature and pristine apparent density. The following conclusions could be obtained.

i Hydrophobic PVF-G_n-H_m sponges have similar apparent densities as the initial hydrophilic PVF samples, exhibit a unimodal macropore size distribution with a peak centered at about 60 μm and high porosity of 90%, maintain the original open-cell pore structure and pore channels well. Their surface hydrophobicity effectively increases with the n-alkyl chain length.

ii In less polar solvents, the Q_s decreases gradually with increasing feed ratio of [GA]/[OH] because the higher crosslinking degree effectively restricts the swelling of samples in these solvents. However, in polar and nonpolar solvents, the hydrophobic sponges show very low Q_s, and no obvious relationship is observed between the absorption performance and the feed ratio of [GA]/[OH].

iii The longer alkyl chain modified sponges possess relatively higher absorption capacities in less polar and nonpolar solvents because of more hydrophobic surfaces and higher solvation degree.

iv The sponges prepared at higher temperature only exhibit slightly increased absorption capacities in less polar and nonpolar solvents because they have higher substitution degrees and exhibit higher solvation degrees. The sponge obtained at ambient temperature also exhibits excellent absorption performance.

v The Q_ss in various solvents decrease with increasing apparent density of pristine sponges, and we believe that the foregoing is related to the higher pore volume during the swelling experiment, i.e., the solvent will occupy the bigger pore volume for the sponge with lower apparent density.

vi As-prepared sponges exhibit excellent reusability during the repeated squeezing–absorption tests and selectivity in water-organic solvent mixture experiment.

As-prepared PVF-G_n-H_ms are easily manufactured, and have high porosity up to 90%, open-cell structure, high absorption performance, good reusability, and selectivity in water-organic solvent mixture, which make them ideal absorbents for solving the problems of chemical leakages and oil spills.

Acknowledgements

This research was supported by National Natural Science Foundation of China (General: 51173180) and Bureau of Science and Technology of Jilin Province (20130206057GX).

Notes and references

1 J. L. Schnoor, *Environ. Sci. Technol.*, 2010, **44**, 4833.

2 H. M. Choi, R. M. Cloud, *Environ. Sci. Technol.*,1992, **26**, 772.

3 E. B. Kujawinski, M. C. K. Soule, D. L. Valentine, A. K. Boysen, K. Longnecker, M. C. Redmond, *Environ. Sci. Technol.*,2011, **45**, 1298.

4 M. O. Adebajo, R. L. Frost, J. T. Kloprogge, O. Carmody, S. Kokot, *J. Porous Mater.*, 2003, **10**, 159.

5 A. Li, H.-X. Sun, D.-Z. Tan, W.-J. Fan, S.-H. Wen, X.-J. Qing, G.-X. Li, S.-Y. Li, W.-Q. Deng, *Environ. Sci. Technol.*,2011, **4**, 2062.

6 I. Karakutuk, O. Okay, *React. Funct. Polym.*, 2010, **70**, 585.

7 X. Gui, H. Li, K. Wang, J. Wei, Y. Jia, Z. Li, L. Fan, A. Cao, H. Zhu, D. Wu, *Acta Mater.*, 2011, **59**,

4798.
8 X. Gui, J. Wei, K. Wang, A. Cao, H. Zhu, Jia, Y.; Q. Shu, D. Wu, *Adv. Mater.*, 2010, **22**, 617.
9. R. A. Venkateswara, N. D. Hegde, H. Hirashima, *J. colloid interface sci.*, 2007, **305**, 124.
10. T. Sun, Y. Guo, W.-C. Li, A.-H. Lu, *Acta Phys-Chim. Sin.*, 2012, **28**, 1432.
11 J. T. Korhonen, M. Kettunen, R. H. A. Ras, O. Ikkala, *ACS Appl. Mater. Interfaces*, 2011, **3**, 1813.
12 D. Ceylan,; O. Okay, *Macromolecules*, 2007, **40**, 8742.
13 O. Okay, S. Durmaz, B. Erman, *Macromolecules*, 2000, **33**, 4822.
14 D. Ceylan, S. Dogu, B. Karacik, S. D. Yakan, O. S. Okay, O. Okay, *Environ. Sci. Technol.*, 2009, **43**, 3846.
15 P. Calcagnile, D. Fragouli, I. S. Bayer, G. C. Anyfantis, L. Martiradonna, P. D. Cozzoli, R. Cingolani, A. Athanassiou, *ACS Nano*, 2012, **6**, 5413.
16 Q. Zhu, Y. Chu, Z. Wang, N. Chen, L. Lin, F. Liu, Q. Pan, *J. Mater. Chem. A*, 2013, **1**, 5386.
17 D. D. Nguyen, N.-H. Tai, S.-B. Lee, W.-S. Kuo, *Environ. Sci. Technol.*, 2012, **5**, 7908.
18 J. Wu, N. Wang, L. Wang, H. Dong, Y. Zhao, L. Jiang, *ACS Appl. Mater. Interfaces*, 2012, **4**, 3207.
19 H. Zhu, S. Qiu, W. Jiang, D. Wu, Zhang, C., *Environ. Sci. Technol.*, 2011, **45**, 4527.
20. J. Lin, Y. Shang, B. Ding, J. Yang, J. Yu,; S. S. Al-Deyab, *Mar. Pollut. Bull.*, 2012, **64**, 347.
21. J. Lin, B. Ding, J. Yang, J. Yu, G. Sun, *Nanoscale*, 2012, **4**, 176.
22 J. Lin, F. Tian, Y. Shang, F. Wang, B. Ding, J. Yu, *Nanoscale*, 2012, **4**, 5316.
23 R. Ltd, *Brit pat. 573,966* Dec, 20, 1945
24 G. P. Ma. A. Gabriel, *Clin. Plast. surg.*, 2009, **36**, 167.
25 D. Queen, J. H. Evans, J. D. S. Gaylor, J. M. Courtney, W. H. Reid, *Burns*, 1987, **13**, 218.
26 M. Kobyahi, H. S. Hyu, *Materials*, 2010, **3**, 2753.
27 P. J. Flory, *J. Am. Chem. Soc.*, 1939, 1518.
28 M. Fernandez, M. Fernandez, P. Hoces., *J. appl. Polym. Sci.*, 2006, **102**, 5007.
29 Y. Pan, W. Wang, C. Peng, K. Shi. Y. Luo, X. Ji, *RSC Adv.*, 2014, **4**, 660.
30 J. M. Schwab, A. Habib, J. B. Klassen, *J. Am. Chem. Soc.*, 1986, **108**, 5304.
31 A. W. Ralston, E. W. Segebrecht, S. T. Bauer, *J. Organ. Chem.*, 1939, **4**, 502.
32 H. G. Hammond,*US 2668153* 1953.
33 O. Okay, *Prog. Polym. Sci.*, 2000, **25**, 711.
34 F. Svec, J. M. J. Fréchet, *Science*, 1996, **273**, 205.
35 A. F. M. Barton, *Chem. Rev.*, 1975, **75**, 731.
36 B. A. Miller-Chou, J. L. Koenig, *Prog. Polym. Sci.*, 2003, **28**, 1223.

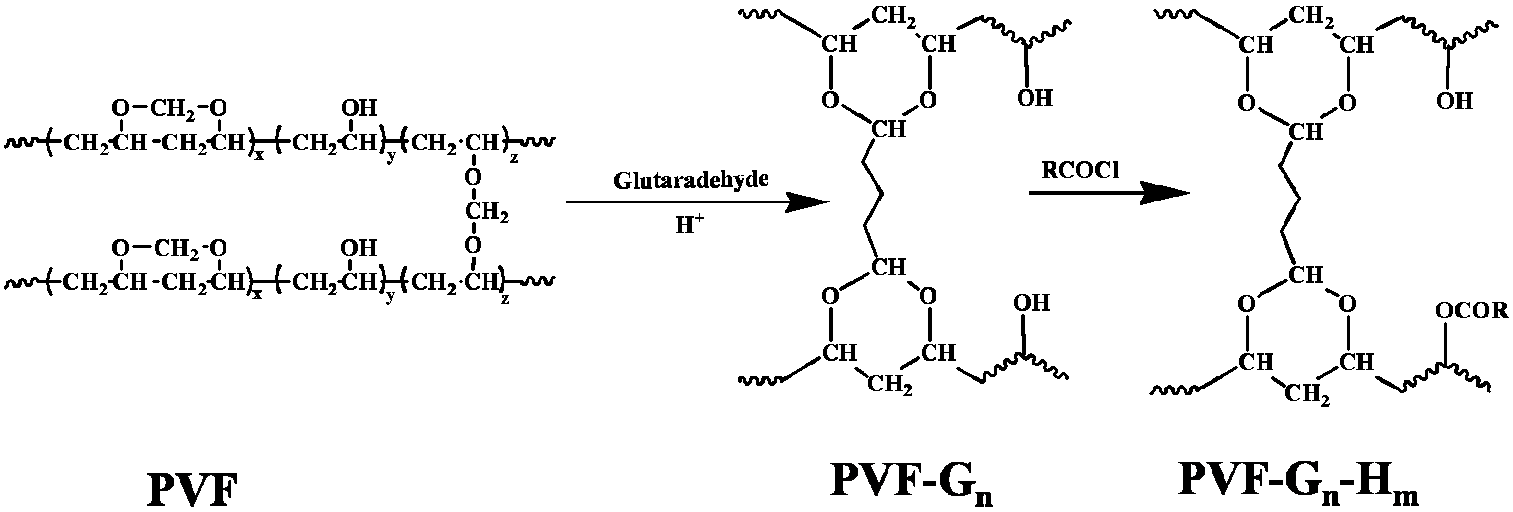

Scheme 1. Synthetic route of PVF–G_n-H_m sponges.

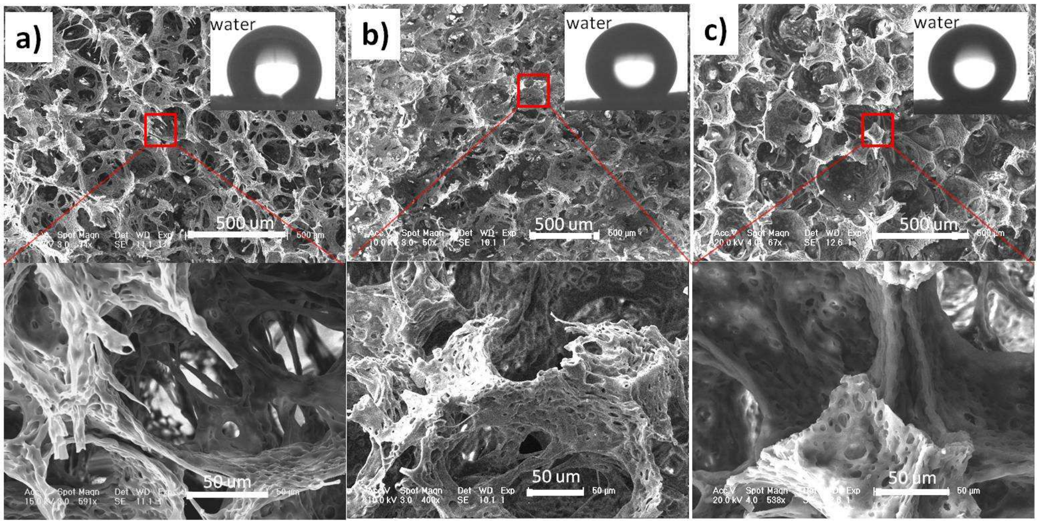

Figure 1. SEM images of PVF samples, (a) PVF-G_1-H_4; (b) PVF-G_1-H_{18}; (c) PVF-G_1-H_{18} (0.110).

(a)

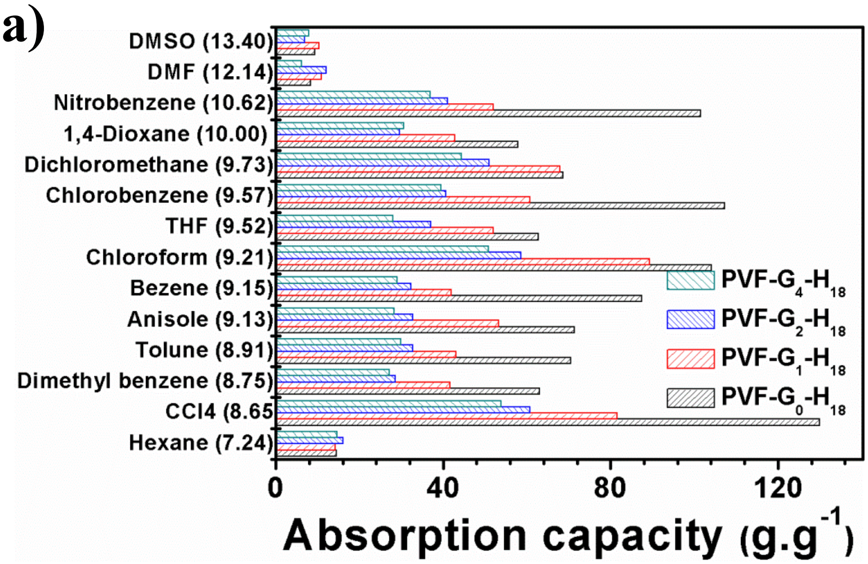
DMSO (13.40)
DMF (12.14)
Nitrobenzene (10.62)
1,4-Dioxane (10.00)
Dichloromethane (9.73)
Chlorobenzene (9.57)
THF (9.52)
Chloroform (9.21)
Bezene (9.15)
Anisole (9.13)
Tolune (8.91)
Dimethyl benzene (8.75)
CCl4 (8.65
Hexane (7.24)
▨ PVF-G$_4$-H$_{18}$
▨ PVF-G$_2$-H$_{18}$
▨ PVF-G$_1$-H$_{18}$
▨ PVF-G$_0$-H$_{18}$
0
40
80
120
Absorption capacity (g.g^{-1})

(b)

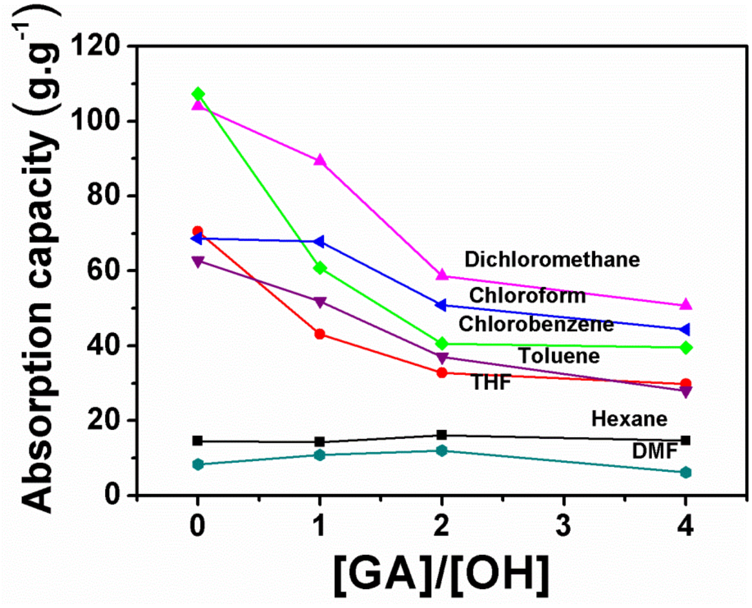
Absorption capacity (g.g^{-1})
120
100
80
60
40
20
0
Dichloromethane
Chloroform
Chlorobenzene
Toluene
THF
Hexane
DMF
0
1
2
3
4
[GA]/[OH]

(c)

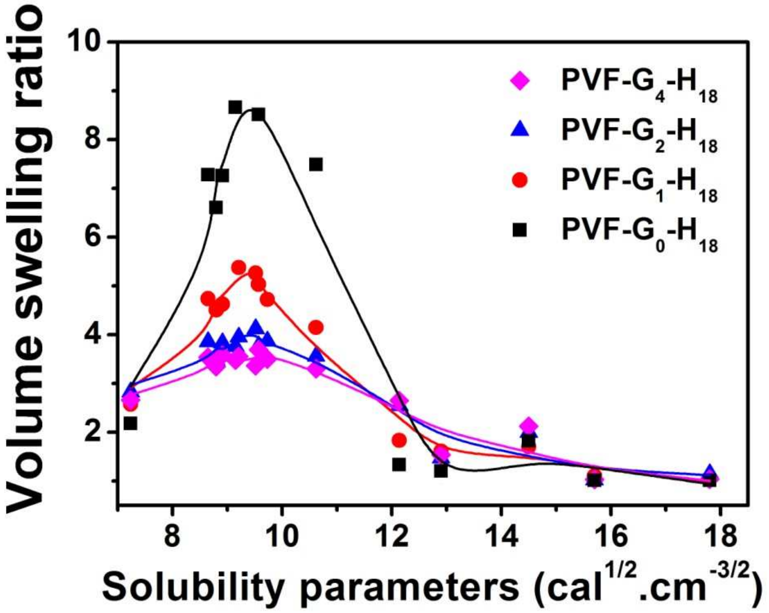

Figure 2. PVF-$G_{0\text{-}4}$-H_{18}s with different feed ratio of [GA]/[OH] in various solvents, (a) absorption capacity; (b) variation of absorption capacity with feed ratio of [GA]/[OH]; (c) variation of volume swelling ratio with solubility parameter of solvents.

(a)

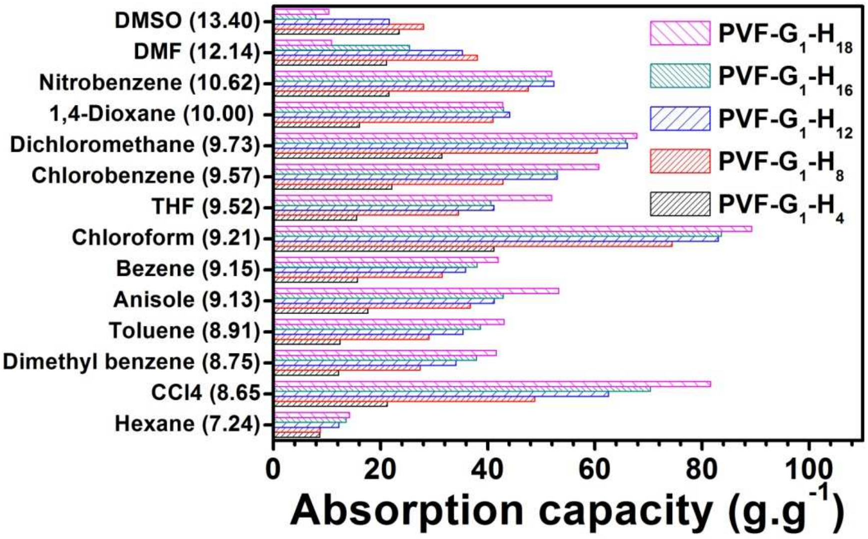
DMSO (13.40)
DMF (12.14)
Nitrobenzene (10.62)
1,4-Dioxane (10.00)
Dichloromethane (9.73)
Chlorobenzene (9.57)
THF (9.52)
Chloroform (9.21)
Bezene (9.15)
Anisole (9.13)
Toluene (8.91)
Dimethyl benzene (8.75)
CCl4 (8.65)
Hexane (7.24)
PVF-G1-H18
PVF-G1-H16
PVF-G1-H12
PVF-G1-H8
PVF-G1-H4
0
20
40
60
80
100
Absorption capacity (g.g-1)

(b)

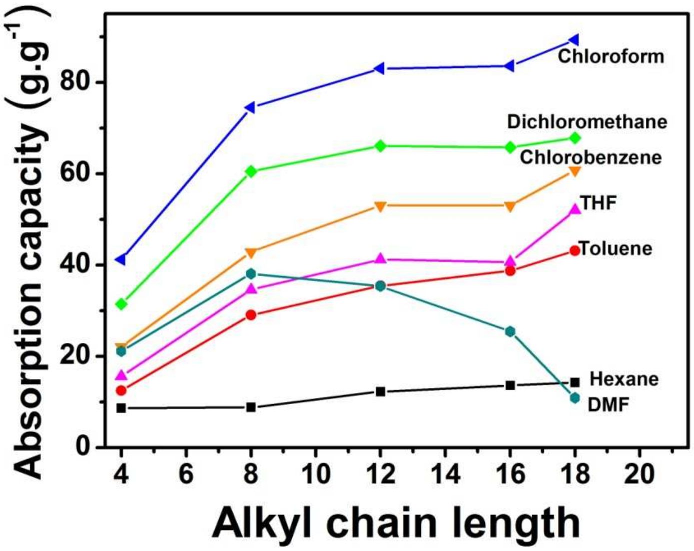
Chloroform
Dichloromethane
Chlorobenzene
THF
Toluene
Hexane
DMF
0
20
40
60
80
Absorption capacity (g.g-1)
4
6
8
10
12
14
16
18
20
Alkyl chain length

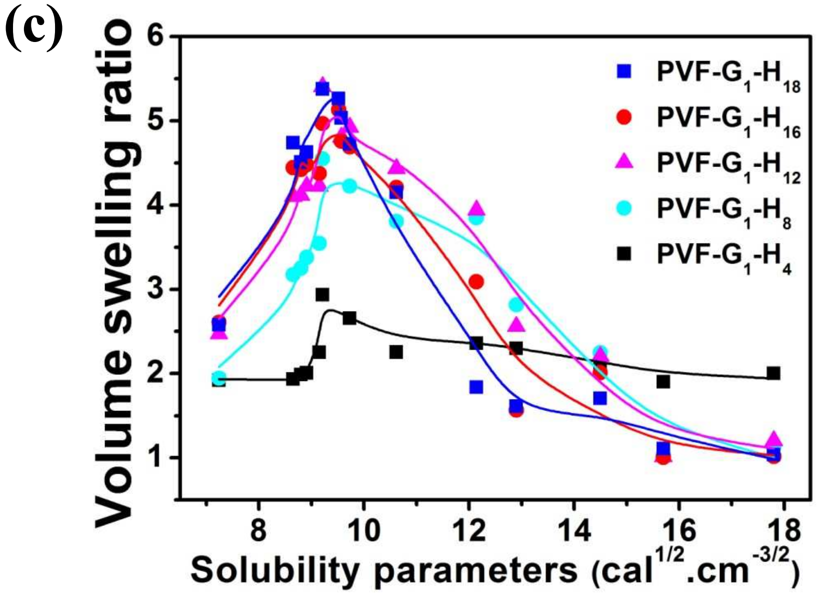

Figure 3. PVF-G_1-$H_{4\text{-}18}$s with different alkyl chain length in various solvents, (a) absorption capacities; (b) variation of absorption capacity with alkyl chain length; (c) variation of volume swelling ratio with solubility parameter of solvents.

(a)

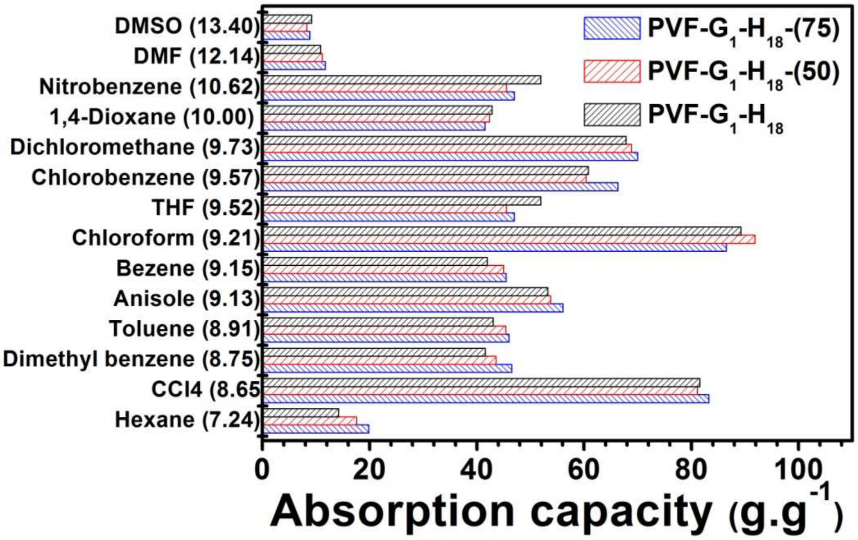
DMSO (13.40)
DMF (12.14)
Nitrobenzene (10.62)
1,4-Dioxane (10.00)
Dichloromethane (9.73)
Chlorobenzene (9.57)
THF (9.52)
Chloroform (9.21)
Bezene (9.15)
Anisole (9.13)
Toluene (8.91)
Dimethyl benzene (8.75)
CCl4 (8.65
Hexane (7.24)
PVF-G$_1$-H$_{18}$-(75)
PVF-G$_1$-H$_{18}$-(50)
PVF-G$_1$-H$_{18}$
0
20
40
60
80
100
Absorption capacity (g.g^{-1})

(b)

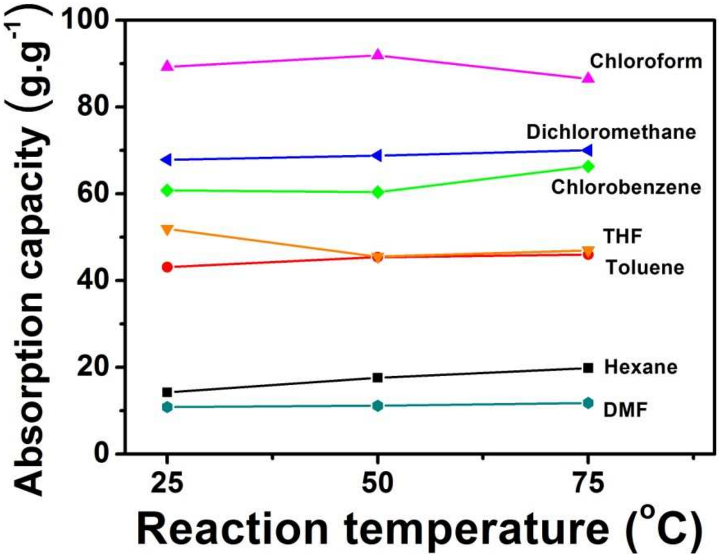
Absorption capacity (g.g^{-1})
100
80
60
40
20
0
Chloroform
Dichloromethane
Chlorobenzene
THF
Toluene
Hexane
DMF
25
50
75
Reaction temperature (°C)

(c)

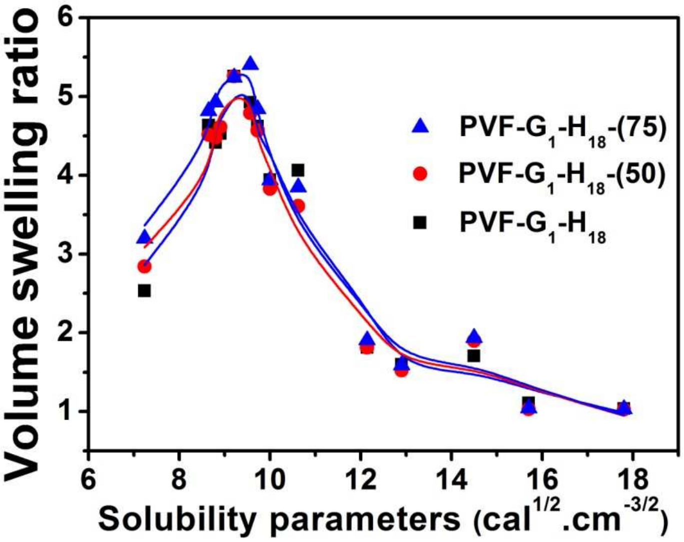

Figure 4. PVF-G$_1$-H$_{18}$s prepared at different reaction temperatures in various solvents, (a) absorption capacity; (b) variation of absorption capacity with reaction temperatures; (c) variation of volume swelling ratio with solubility parameter of solvents.

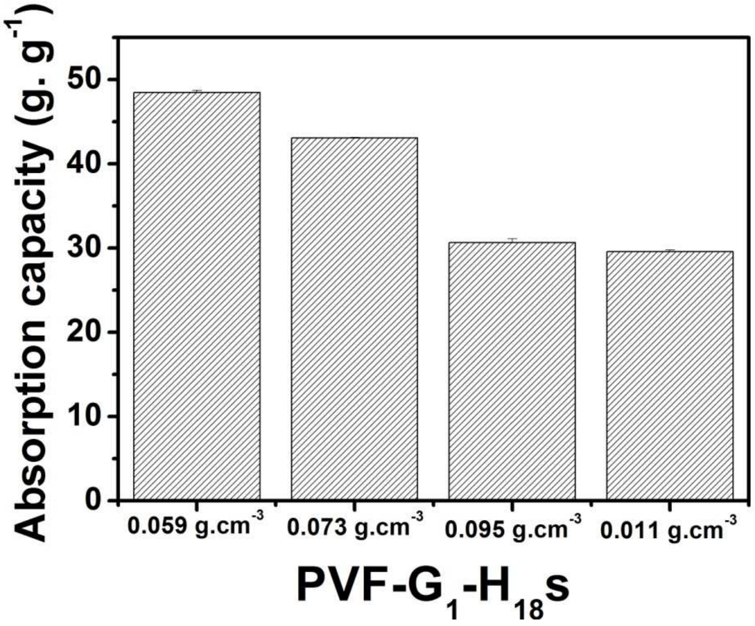

Figure 5. Effect of pristine apparent density on absorption capacities of PVF-G$_1$-H$_{18}$ in toluene.

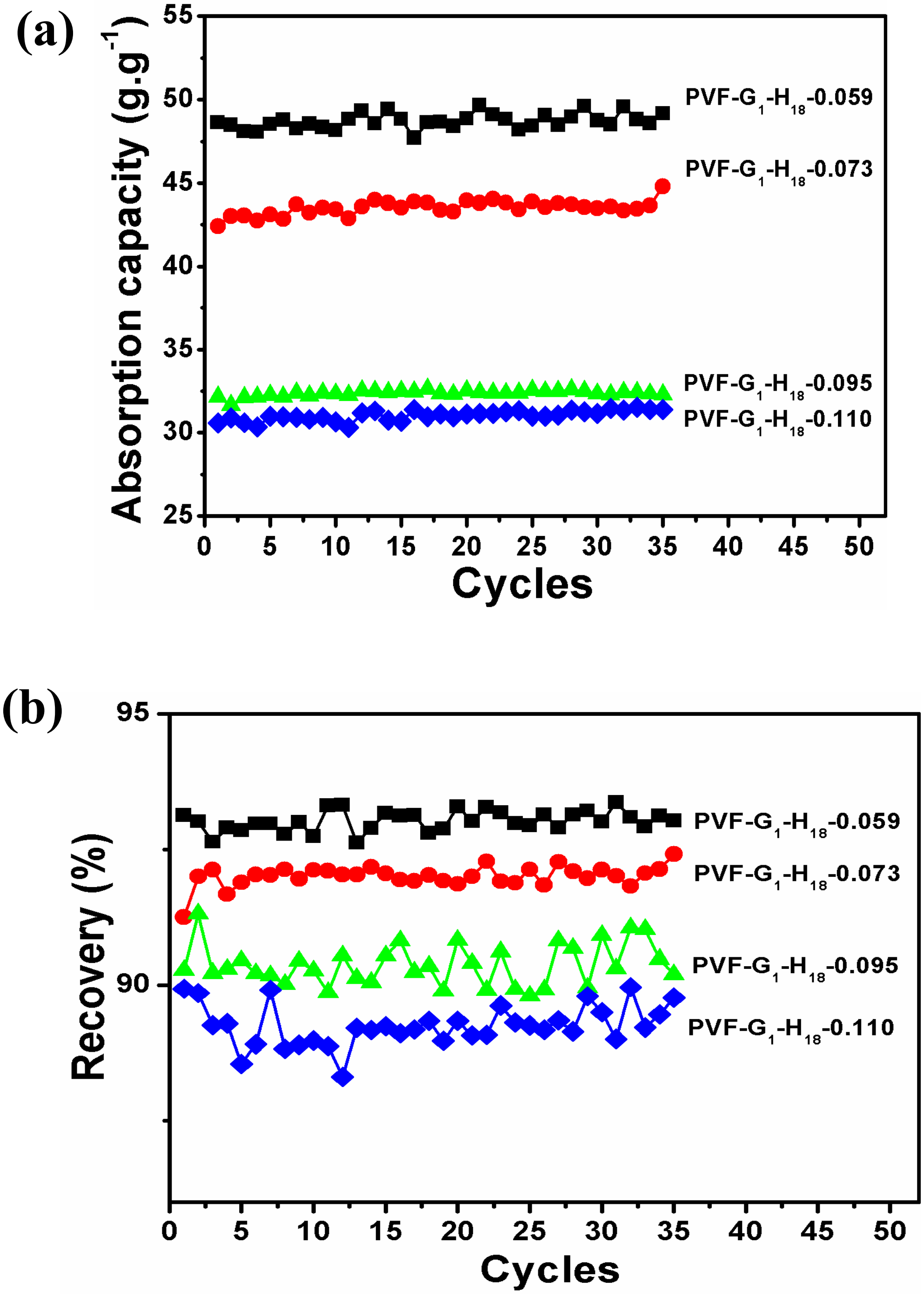

Figure 6 PVF-G_1-H_{18}s with different apparent densities in toluene, (a) reusability, repeated absorption capacity (filled symbols) and residual mass (open symbols); (b) recovery.

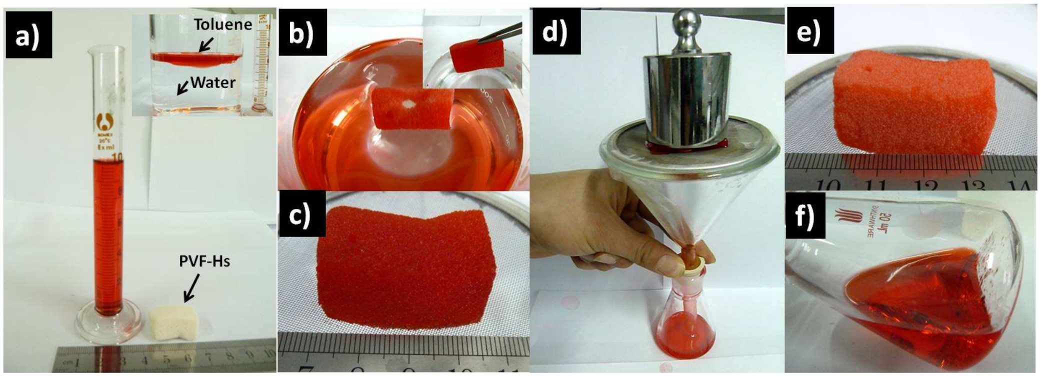

Figure 7. Toluene removal experiment using PVF-G_1-H_{18} (0.095). (a-c) 10 mL toluene was quickly absorbed by sample; (d-f) absorbed toluene was easily recovered by simple squeezing.

Table 1. Physical characterization data for PVFs before and after modification

Samples	Apparent density (g·cm^{-3})	DS[a] (%)	WCA (°)	Porosity[b] (%)
PVF	0.073	——	——	95.0
PVF-G$_1$	0.069	——	——	97.5
PVF-G$_2$	0.070	——	——	——
PVF-G$_4$	0.072	——	——	——
PVF-G$_0$-H$_{18}$	0.077	50.1	132.0 ± 1.0	88.1
PVF-G$_1$-H$_{18}$	0.071	54.1	133.5 ± 0.5	89.7
PVF-G$_2$-H$_{18}$	0.075	45.3	133.3 ± 1.3	92.3
PVF-G$_4$-H$_{18}$	0.071	50.0	132.8 ± 1.0	93.5
PVF-G$_1$-H$_4$	0.070	32.3	123.6 ± 0.9	93.6
PVF-G$_1$-H$_8$	0.071	45.6	124.7 ± 0.8	95.2
PVF-G$_1$-H$_{12}$	0.079	43.3	130.5 ± 0.5	90.1
PVF-G$_1$-H$_{16}$	0.078	44.8	133.5 ± 0.5	92.7
PVF-G$_1$-H$_{18}$（50°C）	0.069	55.0	136.4 ± 0.6	92.8
PVF-G$_1$-H$_{18}$（75°C）	0.073	62.3	138.3 ± 0.7	92.5
PVF-G$_1$-H$_{18}$（0.059）	0.060	55.3	133.1 ± 1.5	90.7
PVF-G$_1$-H$_{18}$（0.095）	0.097	57.8	135.3 ± 1.3	91.4
PVF-G$_1$-H$_{18}$（0.110）	0.114	60.8	136.2 ± 0.8	90.4

a: degree of substitution calculated from the integration of quantitative solid-state CP/MAS ^{13}C NMR spectra

b: measured by mercury intrusion porosimetry

TOC

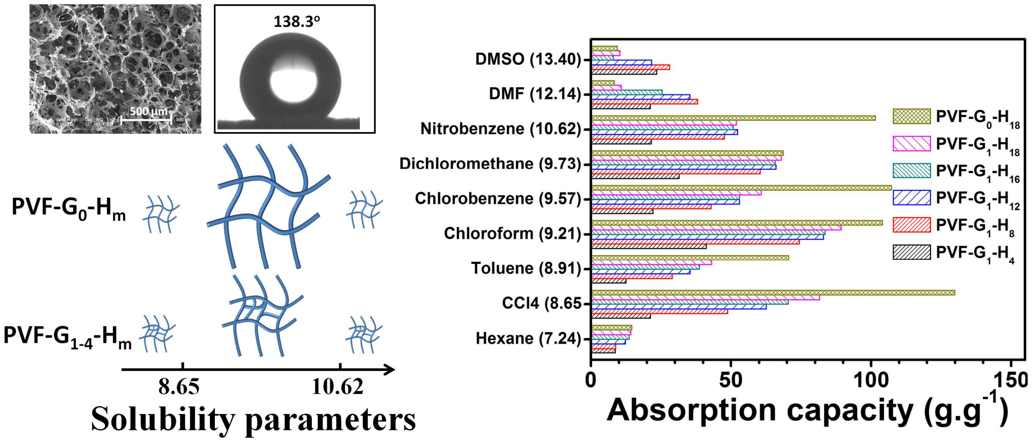
500 μm
138.3°
PVF-G$_0$-H$_m$
PVF-G$_{1-4}$-H$_m$
8.65
10.62
Solubility parameters
DMSO (13.40)
DMF (12.14)
Nitrobenzene (10.62)
Dichloromethane (9.73)
Chlorobenzene (9.57)
Chloroform (9.21)
Toluene (8.91)
CCl4 (8.65
Hexane (7.24)
PVF-G$_0$-H$_{18}$
PVF-G$_1$-H$_{18}$
PVF-G$_1$-H$_{16}$
PVF-G$_1$-H$_{12}$
PVF-G$_1$-H$_8$
PVF-G$_1$-H$_4$
0
50
100
150
Absorption capacity (g.g^{-1})